Physical Chemistry 2016, 6(2): 39-48
DOI: 10.5923/j.pc.20160602.02

Removal of Methyl Orange (MO) from Water by adsorption onto Modified Local Clay (Kaolinite)

Fortunate Phenyo Sejie, Misael Silas Nadiye-Tabbiruka*

Department of Chemistry, University of Botswana, Gaborone, Botswana

Abstract The kinetics and thermodynamics of the removal of methyl orange from water, by using kaolinite clay from Lobatse, was investigated spectrophotometrically using the batch technique. The adsorption rate and the capacity increased with increasing initial MO concentration, with decreasing solution pH and with decreasing temperature indicating a physisorption process. The adsorption kinetics data fitted the pseudo second order model best. However, the possibility of a three body collision mechanism at the rate determining step was discounted on grounds of very low probability. Instead two simultaneous two body collisions mechanism at the rate determining step was preferred as it has a higher probability. The two simultaneous body collisions were identified as the adsorption of the dye on the external, and on the internal surfaces of Lobatse clay. The external surface is thought to be the virgin unhidden surface while the internal surface is either in pores or in the narrow gaps between adsorbed molecules on the pre-adsorbed surface. Results from the thermodynamic study fitted the Freundlich model best indicating heterogeneity of the surface of the clay sample.

Keywords Adsorption, Methyl orange, Lobatse clay, Kinetics, Thermodynamics

1. Introduction

Purification of water can be achieved by using a variety of methods including coagulation, flocculation, ozonation, reverse osmosis, and adsorption [1]. The method of choice is determined by the type of contaminant to be removed. Several water contaminants/pollutants are chemicals that are useful in industries like pharmaceutical, food, laboratory printing and textile industries [2-6]. Organic compounds are major pollutants used in the mentioned industries especially the synthetic dyes. A variety of azo dyes find use in the food and textile industries. However, most of these dyes are highly carcinogenic even when present in minute quantities.

Methyl orange is a carcinogenic water soluble azo dye which is widely used in textile industries, in manufacturing printing paper, and in research laboratories. It is also metabolised into aromatic amines by intestinal microorganisms [7, 8]. Methyl orange is stable, shows low biodegradability and is soluble in water hence it is difficult to remove from aqueous solutions by common water purification/treatment methods [9]. Clays contain minerals which are responsible for their properties. Clay minerals are widely used in several industries and fields such as in polymers nano-composites adsorbents fields, in heavy metal ion adsorption, ceramics, and paper fillings [10-12]. These minerals are made up of tetrahedral and octahedral layers and hence they are characterised by the ratio of this sheets/ layers in the structure. A clay made up of 2 tetrahedral sheets and 1 octahedral sheet it is referred to as a 2:1 clay type (3 sheets) while those with 1 octahedral sheet and 1 tetrahedral sheet are called 1:1 (2 sheets) clay types [13-19]. Clay minerals in soil may play a role in scavenging of pollutants from water. The commonly used clays include montmorillonite, semectites kaolinite and illite.

* Corresponding author:
nadiyemst@yahoo.com (Misael Silas Nadiye-Tabbiruka)
Published online at http://journal.sapub.org/pc

2. Experimental

2.1. Materials

2.1.1. The Adsorbent

The powdered clay obtained from Lobatse Clay Works which is near Lobatse town in southern Botswana, was mixed with excess deionised water and stirred for 48 hours. It was then allowed to settle for 24 hours. The top water layer as well as the top fine particles were decanted and filtered under vacuum. The clay was leached with 2M Oxalic acid for 2 hours at 371K to remove metal ferrous ions which absorb at the same wavelength as the investigated dye. The acid was filtered off and the clay was washed with deionised water until the filtrate no longer formed a precipitate with sodium hydroxide. The Clay was dried in an oven at 383.15K and stored in a desiccator. FTIR, ESEM and XRPD analysis techniques were employed to characterise the powder.

2.1.1.1. Characterisation of the Adsorbent

X-Ray Powder Diffraction

The spectrum shows the clay to be highly crystalline as the peaks are narrow. The main peaks at 2θ=20.89° and 26.65° are characteristic bands for quartz SiO_2 which is a silica polymorph consisting of interconnected SiO_2 tetrahedral that build up a rigid three-dimensional network. The peak at 2θ=12.41° and 50.13° are characteristic of a kaolinite clay mineral. From this XRPD analysis, Lobatse clay is a crystalline silicate Kaolinite of chemical formulae $Al_2Si_2O_5(OH)_4$ mixed with interconnected quartz SiO_2. The identified phases are represented in table 1 below.

Table 1. Identified clay phases

Compound Name	Chemical Formula
Quartz low	SiO_2
Kaolinite	$Al_2Si_2O_5(OH)_4$

Scanning electron microscope

Figures 2a and b show flake clustered particles which are irregular in shape, have a smooth irregular surface.

Fourier Transform Infra-Red

Figure 3 shows the FTIR spectra of Lobatse clay. The bands at 3696.5cm^{-1} and 3619.98 cm^{-1} are assigned to the coupled OH stretching mode from IR tables for clays. These are the 2 coupled hydroxyl groups that are characteristic of the kaolinite clay minerals. The band at 3619.98cm^{-1} lies wholly within the kaolin layers with the proton end directed towards the octahedral repeat layers. The other hydroxyl band at 3695.5cm^{-1} is positioned in a way that allows hydrogen bonding to the oxygens from the adjacent repeat layer, also the dipoles of this hydroxyl group are perpendicular to the surface of the crystal, giving a negative overall charge of the surface of the clay. The Si-OH and Si-O$^-$ bending respectively are found at 1023.05cm^{-1} and 1005.17cm^{-1} respectively. The Al-Al-O deformation asymmetric stretch is found at band 912.04 cm^{-1}. The Al-O-Si inner vibration observed at 797.38cm^{-1} is due to the presence of quartz in the clay sample. This is also supported by the presence of the band at 696.35cm^{-1}.

The FTIR information above correlates with the XPRD data on figure 1.

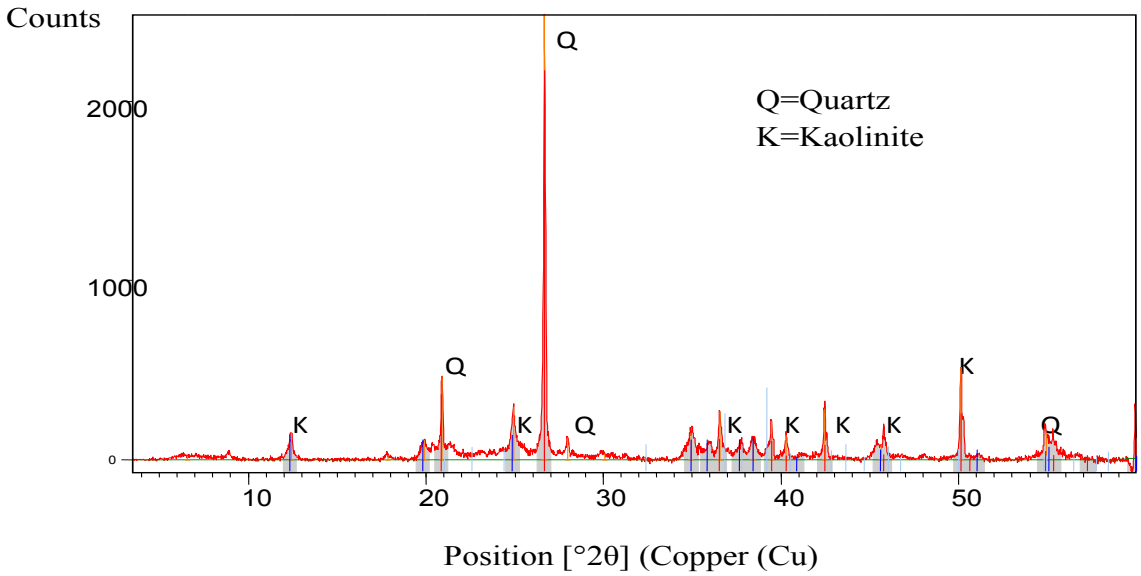

Figure 1. Shows the XRPD spectrum of Lobatse clay

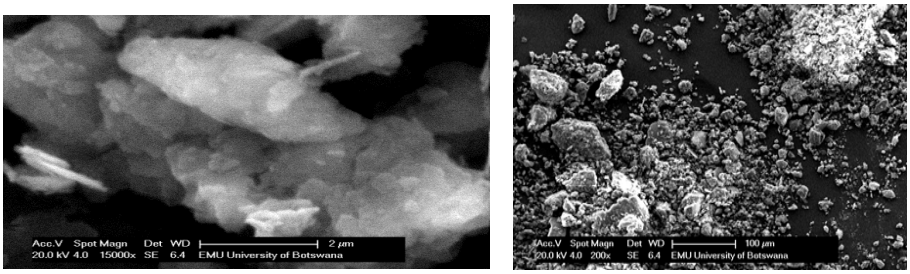

a b

Figure 2. a and b SEM micro structures of Lobatse clay

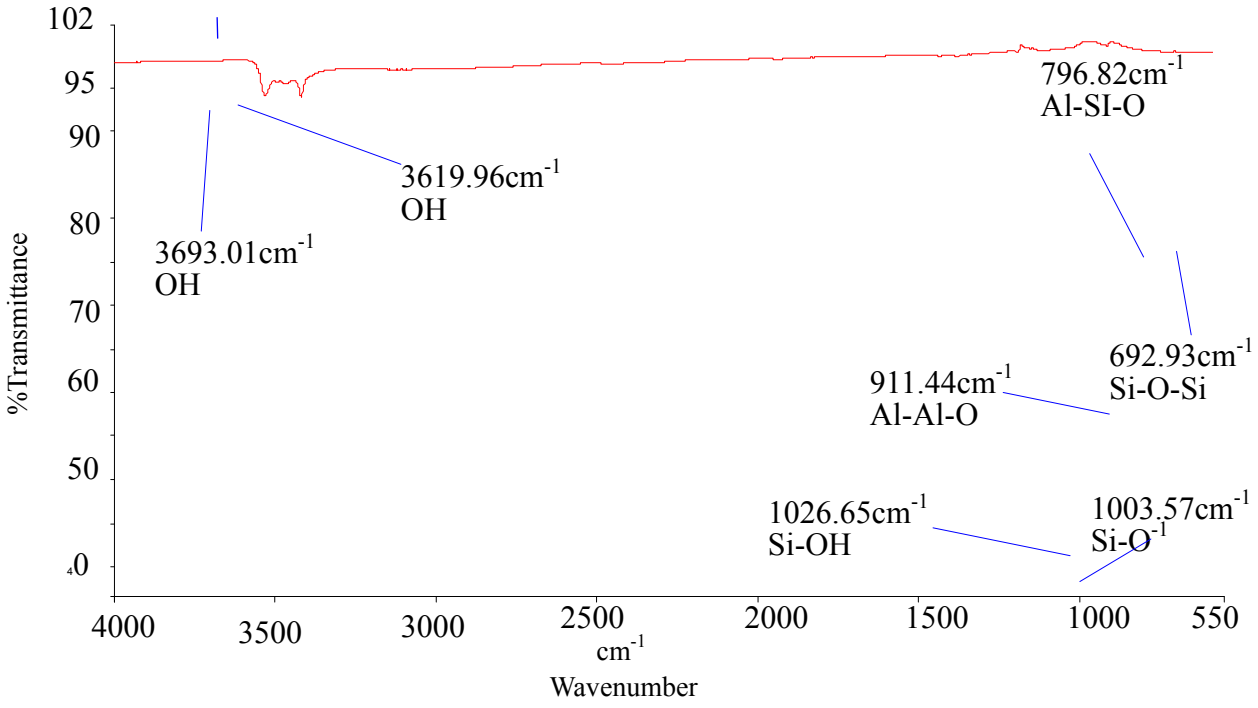

Figure 3. FTIR Spectrum of Lobatse clay

2.1.2. The Adsorbate (methyl orange MO)

Methyl orange (Anionic, water soluble azo dye) powder ($C_{14}H_{14}N_3NaO_3S$, figure 4) supplied by SAARCHEM, South Africa was used without any further purification. A solution of the dye was made by dissolving a known weight into double distilled de-ionised water. Other required dye concentrations were prepared by serial dilution. Several of these concentrations were used to obtain calibration a curve of absorbance against concentration at a predetermined wavelength at maximum absorbance λ=463 nm using a UV-Visible spectrophotometer spectronic 20. This wavelength was determined by scanning and plotting the absorbance for all the wavelengths on the machine using methyl orange solution. Measurements of absorbance at a wavelength maximum improves the sensitivity and hence the accuracy of the machine. Exact concentrations were then determined from this calibration curve

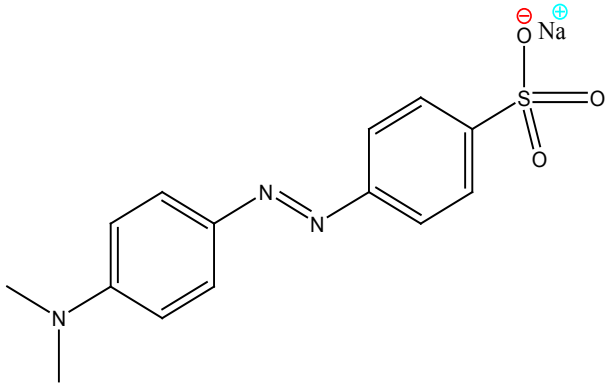

Figure 1. Methyl orange structure

2.2. Procedure

2.2.1. Adsorption Kinetics' Studies

1.5g of powdered clay was added to 150ml of MO solution in a screw capped bottle contained in a water bath at constant temperature, and adsorption time was recorded. Samples of the supernatant liquid were drawn off after predetermined time intervals, filtered using an appropriate filter paper and their absorbance were taken using a UV/VIS spectrophotometer at a wavelength of 463 nm. The amount adsorbed was obtained by difference from the initial concentrations and plotted against time. The experiment was repeated for various MO concentrations, reaction temperature and pH.

2.2.2. Adsorption thermodynamics Studies

In this section, a batch technique was used. Lobatse clay (0.5 g) was added to each of several 250 mL screw capped bottles containing 50 ml of methyl orange of different initial concentrations. The bottles were kept in a thermostatic water bath shaker at a speed of 220 rpm for 3.8 hours at constant temperature. After the samples had reached equilibrium, the Solutions were filtered using 0.45 µm filter paper and their residual concentrations were determined spectrophotometrically as before. The amount adsorbed at equilibrium, q_e (mol/g), was calculated by using equation 1 below:

$$q_{e=}[\frac{(C_0-C_t)}{m}] * V \quad (1)$$

Where C_o is the initial concentration of the dye and C_t is the concentration of the dye after time t (Minutes) (mol/L), V

(L) is the volume of methyl orange solution and m (g) is the weight of Lobatse clay. The equilibrium adsorption q_e values were used to plot an adsorption isotherm.

3. Results and Discussion

3.1. Adsorption Kinetics Analysis

3.1.1. Lagergren Pseudo 1st Order Model

Lagergren first-order rate equation is the earliest known model describing the adsorption rate based on the adsorption capacity [21]. The equation representing this model is:

$$\log(q_e - q_t) = log q_e - \frac{k_1}{2.303} t \quad (2)$$

Where k_1 is the pseudo first order rate constant in g/mg* min

q_e is the amount adsorbed at equilibrium

q_t is the amount adsorbed at time t

t is the time

A plot of $\log((q_e - q_t))$ against t will give a straight line and k_1 can be determined from the slope and q_e from the intercept. The straight line shows that adsorption onto the adsorbate (solid) follows the pseudo first order model kinetics. The parameters that can be derived from this model are the rate constant the theoretical and the equilibrium amount adsorbed q_e.

Figure 5 show the Lagergren pseudo first order model plot for MO adsorption onto Lobatse clay at various temperatures. The plot gives two straight line segments for the temperature range 288K-318K indicating that two processes are operating. There is a faster process dominating the period from 0-5 minutes then a slower process which dominates thereafter. The first section can be related to the binding of methyl orange to the most active sites on the external surface of the adsorbents while the second longer linear segment can be associated to the same process that is pseudo first order kinetics of adsorption of the dye molecules onto the internal or less accessible surface of the adsorbents [22-28].

3.1.2. Lagergren Pseudo Second Order Model

Pseudo-second-order rate expression is mostly used in an attempt to describe adsorption process. It has been widely applied to the adsorption of pollutants from aqueous solutions.

This model is represented by the equation

$$\frac{dq_t}{d_t} = k_2 (q_e - q_t)^2 \quad (3)$$

A linear form of this equation is

$$\frac{t}{q_t} = \frac{1}{k_2 q_e^2} + \frac{1}{q_e} t \quad (4)$$

Where k_2 is the pseudo first order rate constant in mol/g min

q_e is the amount adsorbed at equilibrium

q_t is the amount adsorbed at time t

t is the adsorption time

This equation is only applicable if a plot of $\frac{t}{q_t}$ against t gives a straight line from which k_2 and the theoretical equilibrium amount adsorbed can be determined. The fitting of the kinetics data onto the pseudo second order is shown in Figure 6.

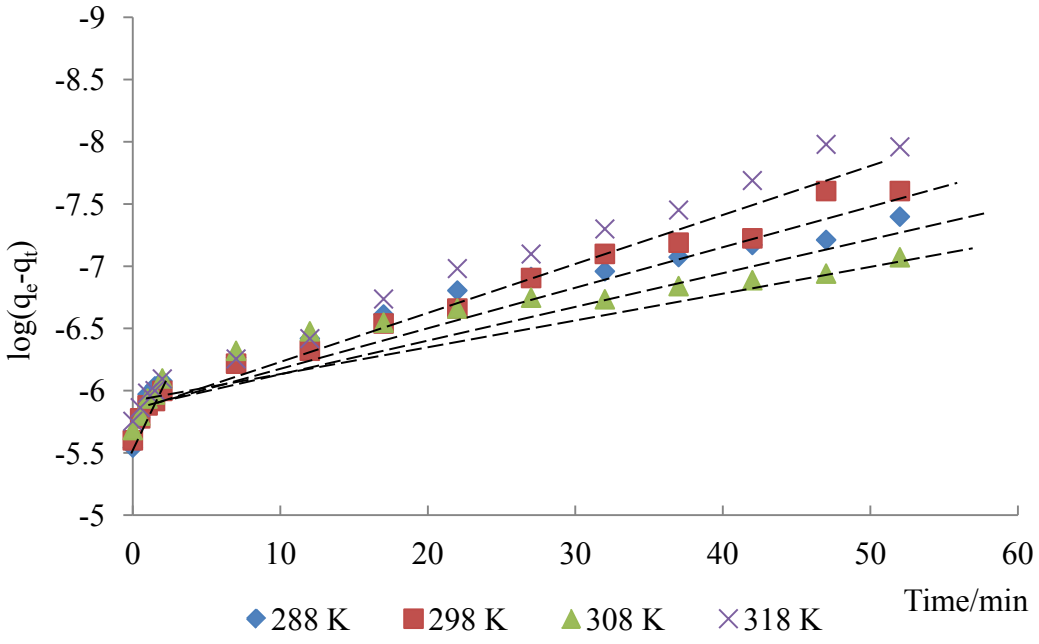

Figure 2. Lagergren pseudo first order plot for MO adsorption onto Lobatse clay

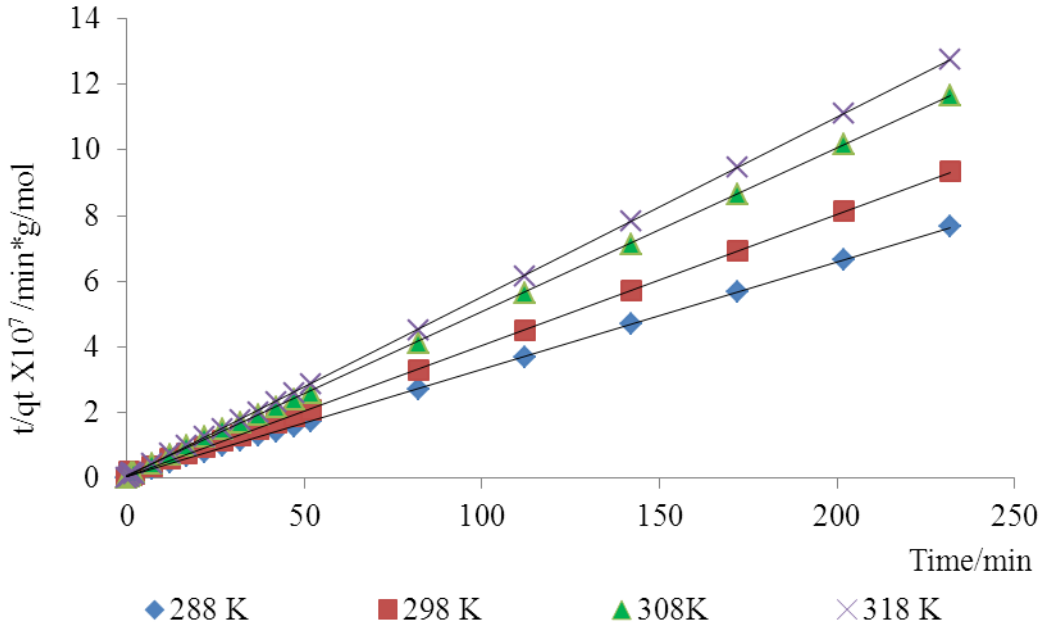

Figure 3. Lagergren pseudo second order Kinetic model plot for the adsorption of methyl orange onto Lobatse clay 5.49 × 10^{-5} M pH 7.18 10 g/L sorbent dosage

The straight lines fit from the beginning of the sorption process to the end without an intercept. The data fit onto this model is good suggesting that the adsorption process onto the adsorbent is overall third order which implies that the rate determining step in the mechanism involves three bodies colliding at the same time (for instance two methyl orange molecules and an adsorption site or one methyl orange molecule, a solvent molecule and an adsorption site). However, the probability of such a collision is very low and hence the mechanism is unlikely. This leaves only one option that is a mechanism constituting a combination of two simultaneous body collision processes. These are identified in this work as the combination of adsorption of methyl orange on the external and on the internal surfaces of the clay which were detected earlier from the pseudo first order model fitting. Similar observations were made in the study of bio sorption of yellow 4GL onto kaolinite [29], methylene blue and Congo red onto activated carbon, humic and tannic acid onto chitosan [30], and methyl orange onto Carbon nano tubes [31].

3.1.3. Effect of Varying Concentration on the Adsorption Process

The effect of varying concentration on methyl orange adsorption kinetics was investigated in the concentration range 1.02×10^{-4} M to 1.56×10^{-5} M, at pH 7.18, 298K and sorbent dosage of $10gL^{-1}$. Figure 7 presents the kinetics data at 298K. Clearly, at all concentrations, the process is at equilibrium within fifty minutes, with the higher concentrations taking longer and giving a higher adsorption capacity than the lower concentrations.

Three higher concentrations have close adsorption capacities compared to the lowest concentrations. It is qualitatively clear from the slopes of the curves for both adsorbents that increasing the initial concentration of methyl orange solution increases the rate of adsorption of the dye. The process is initially rapid but slows down as equilibrium adsorption approaches. The increase in rate with increasing initial concentration can be attributed to an increase in the driving force or increased concentration gradient in accordance with the law of mass action, in the range 1.02 x 10^{-4}M to 1.56 x 10^{-5}M. The initial concentration provides a driving force to overcome the effect of mass transfer resistance to adsorbate (methyl orange) by the aqueous solution and solid adsorbent phase. This can also be explained in terms of the presence of large number of easily accessible vacant sites of the adsorbent for adsorption at the beginning of the process, but after a while, the remaining sites are fewer and less accessible because of the repulsive forces between the dyes molecules on the surface and the un-adsorbed dye molecules as well as the structure of the adsorbent.

3.1.4. Effect of Varying Temperature on the Adsorption Process

Increase in the temperature from 288K-318K lead to a decrease in the adsorption capacity, as shown in figure 8, indicating possibilities of reversible adsorption process [20].

3.1.5. Effect of Varying pH on the Adsorption Process

A change in the pH of the solution affects both the dye structure and the surfaces of the adsorbent. This should in turn lead to a change in the adsorbents sorption rate and capacities.

As seen in figure 9 the adsorption of methyl orange onto the clay increases as pH is lowered from 12 to 4.

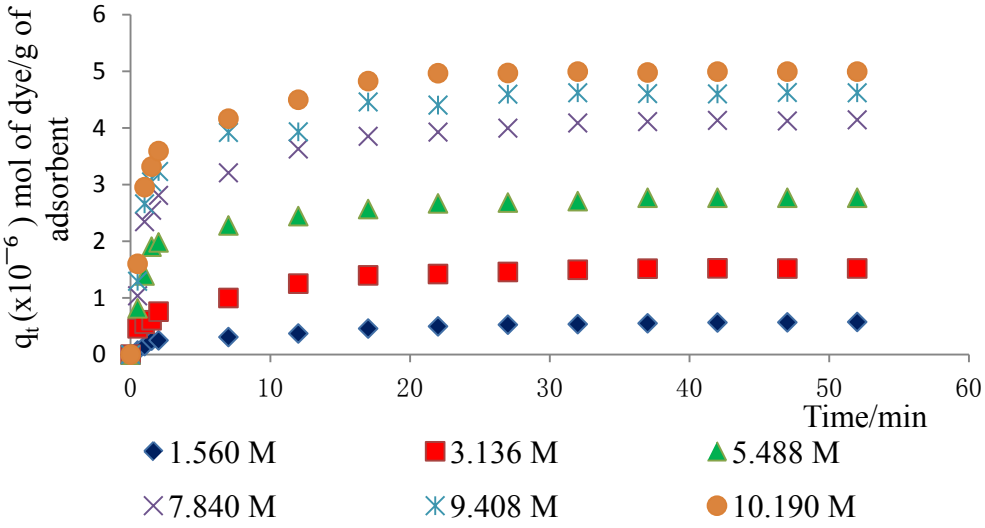

Figure 7. Effect of varying initial molar concentrations on the adsorption of MO onto Lobatse clay at 298K, pH 7.18 and sorbents dosage of 10gL^{-1}

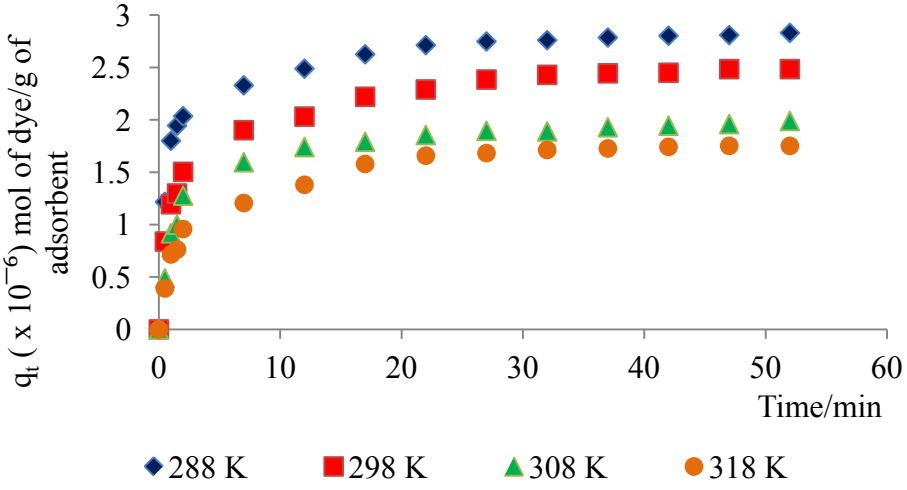

Figure 8. Effect of Temperature (K) on the adsorption of methyl orange onto Lobatse clay, 5.49× 10-5 M, pH 7.18 and sorbent dosage 10gL^{-1}

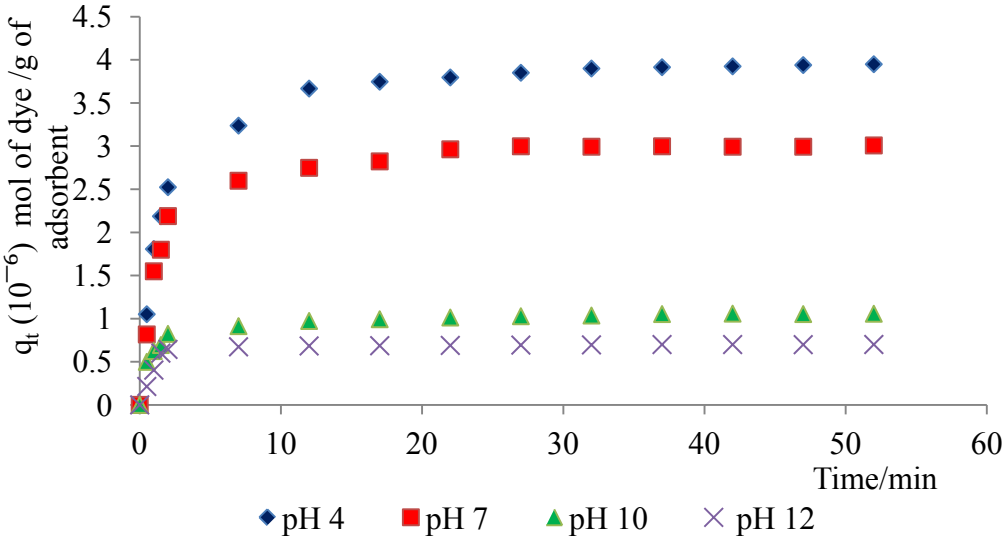

Figure 9. Effect of varying pH on the adsorption of Methyl Orange onto Lobatse clay 5.49× 10^{-5} M, 298 K and sorbent dosage 10gL^{-1}

3.1.5.1. Effect of pH on the Structure of the Dye

As pH is increased to more basic conditions, the double bond conjugation is lost and a proton is lost, and the molecule rearranges to form a negatively charged species (figure 10a). The positive charges have been neutralized. Due to excess anions in the solution, there will be repulsion of the dye by the negatively charged surfaces of the adsorbents, also an increase in pH leads to the modification of the pi (Π) system delocalization pattern. In the literature, the uptake of methyl orange on several adsorbents was similarly found to be favoured at lower pH (acidic medium). Furthermore, at lower pH, the surface of the adsorbent was found to be activated by the acid in solution and the dye became protonated thus enhancing adsorption process.

At lower pH Methyl orange assumes the structure shown in figure 10.

3.1.5.2. Effect of pH on the Structure of the Dye

As the pH is increased to more basic conditions, the double bond conjugation is lost and a proton is lost, and the molecule rearranges to form a negatively charged species as shown in figure 8 above. The positive charges have been neutralized. Due to excess anions in the solution, there will be repulsion of the dye by the negatively charged surfaces of the adsorbents.

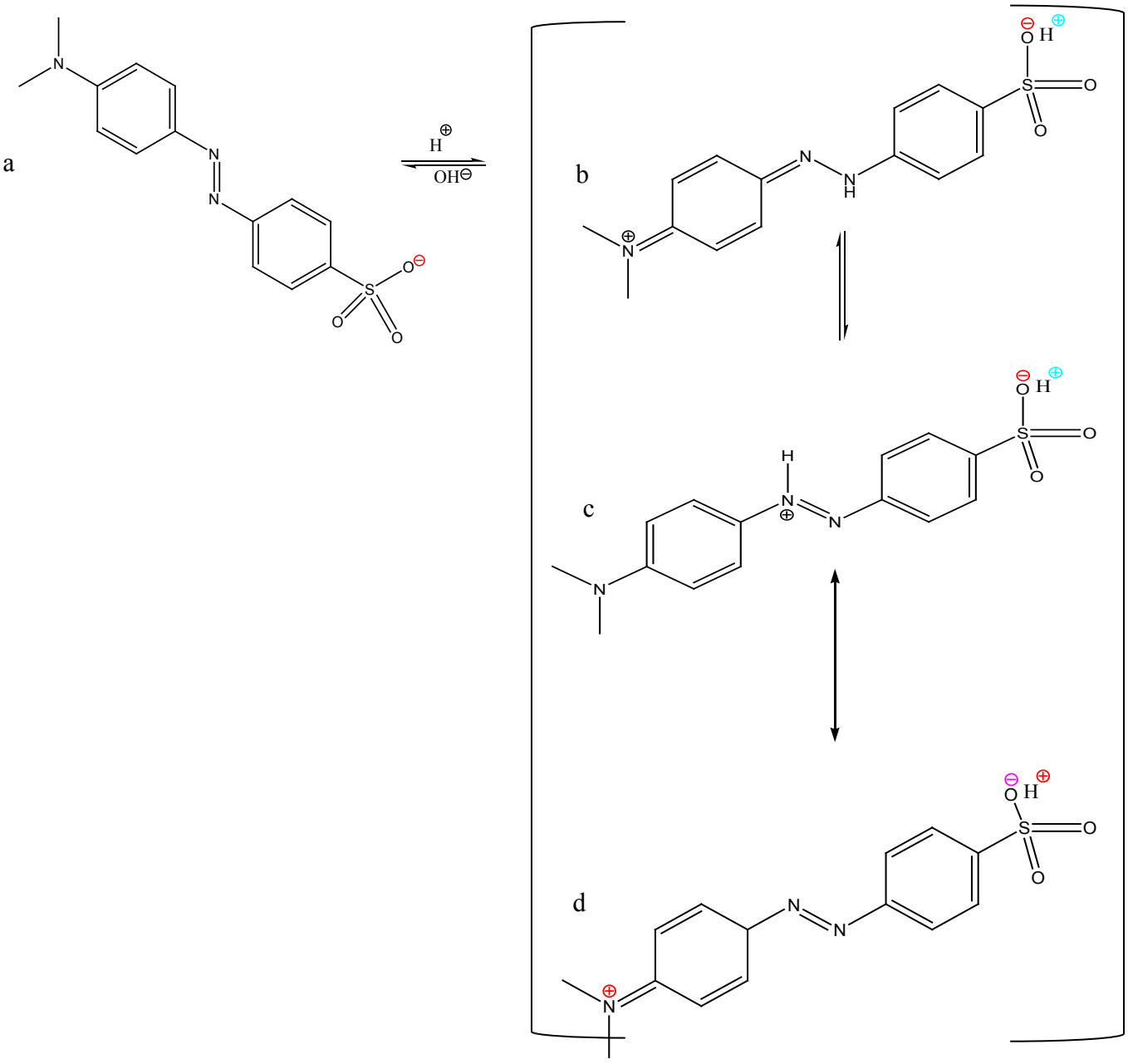

Figure 10. Alkaline form of Methyl orange (a) and its mono-protonated zwitter ionic structures under acidic conditions (b, c and d)

3.2. Thermodynamics' Analysis

Interaction of adsorbate with adsorbents can be investigated by plotting adsorption isotherms. In the current case equilibrium adsorption is plotted against concentration at constant temperature. The data obtained can then be fitted on various models to obtain a comprehensive understanding of the nature of the interactions involved.

3.2.1. Freundlich Isotherm

Freundlich (1906) established an empirical relationship between the equilibrium amounts adsorbed q_e and their equilibrium concentrations C_e. It has now been shown to represent non-ideal adsorption onto heterogeneous surfaces of adsorbents; thus:

$$q_e = K_f\, {c_e}^{1/n} \tag{5}$$

The linear form of equation 5 is:

$$lnq_e = lnK_f + \frac{1}{n} lnc_e \tag{6}$$

Figure 11 shows a reasonable fit to Freundlich model plot for the adsorption of the dye onto the clay, which indicates that adsorption of methyl orange onto the clay took place on a heterogeneous surface. It also indicates that the process of adsorption is reversible.

3.2.2. Temkin Model

Temkin and Pyzhev's adsorption model based on the effect of indirect adsorbent -dye interactions on adsorption leads to, the heat of adsorption of all the molecules in a layer decreasing linearly with surface coverage.

The quantity adsorbed at equilibrium q_e is related to equilibrium concentration c_e by the equation 7 below Which linearizes to equation below. And a plot of q_e against ln C_e gives the heat of adsorption from the slope and the equilibrium binding constant from the intercept. A small value of the parameter b model indicates a physisorption process.

$$qe = \frac{RT}{b} \ln A_t + \left(\frac{RT}{b}\right) lnc_e \tag{7}$$

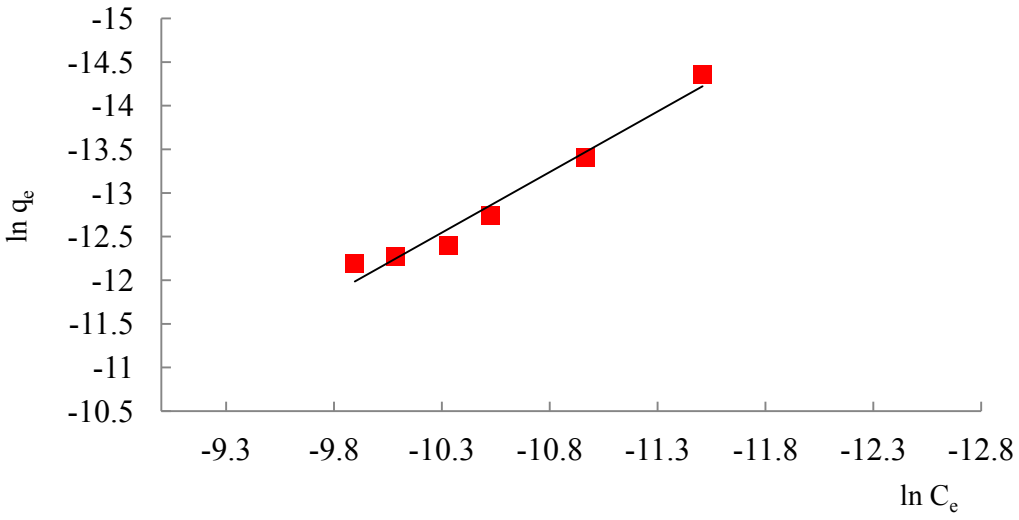

Figure 4. Freundlich Isotherm for the adsorption of Methyl orange Lobatse clay

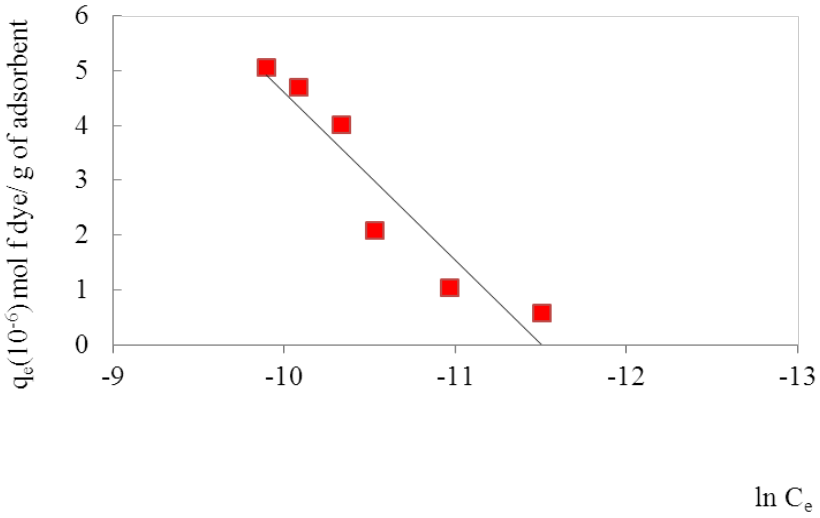

Figure 5. Temkin model for the adsorption of the dye onto the clay

Figure 12 above shows the fitting of adsorption data on the Tempkin at 298K. The data fits the Temkin model well for Lobatse clay.

Table 2. Thermodynamics isotherm parameters

Adsorption Model	Parameter	Value
Freundlich	k_f (mol/{g/L}$^{1/n}$) x10^{-2}	5.7730
	$\frac{1}{n}$ (g/L)	1.3880
	R^2	0.9671
Temkin	K_t/A_t (L/g)E05	1.1028
	B E-6 j/mol	2.9800
	R^2	0.9723

Table 3 was obtained from figure 11 and 12 above. From table 3 the correlation coefficients confirm reasonable fitting. The constant b, related to heat of adsorption is very small for the adsorbent indicating a physical adsorption process [32-35].

Table 3 above, also shows good fitting on the Freundlich isotherm model (correlation coefficients R^2>0.96) indicating heterogeneity of the adsorbents, as was expected. The relative adsorption capacity k_f was found to be 5.7730. The heterogeneity factor ($\frac{1}{n}$) was found to be 1.3880. This value is higher than 1 which indicates cooperative adsorption [36-38], and confirms heterogeneity which probably originates from the rough irregularities of the surface as shown by the SEM micrograms (see Figure 2).

4. Conclusions

It was found that adsorption attains equilibrium within 50 minutes. The adsorption rate process is best described by the Lagergren pseudo second-order rate model. Adsorption of Methyl orange onto the clay increases with decreasing temperature, with decreasing pH and with increasing concentration, as expected from the law of mass action, in the range studied. The decrease of adsorption with increasing temperature is thought to be due to weak attraction between the dye molecule and the surface originating from the weak Van der Waal's forces. This is indicative of physical adsorption. The increase of adsorption with decreasing pH is believed to originate from the increased concentration of MO cationic species resulting from the protonation of the nitrogen atoms in the MO molecule in acid conditions. It is recommended that the surface area and pore-size distribution of the clay be obtained from nitrogen gas adsorption to gage its current capacity and then improve on it as well as on the accessibility of the adsorbent by activation and grinding the clay to nano particle size. This will not only increase its surface charge density but also its accessible surface area and porosity thus enhancing its water purification application.

ACKNOWLEDGEMENTS

The authors wish to acknowledge the services and contributions from the University of Botswana, Department of Chemistry for financing this research project and providing laboratory space. The contribution from the technical staff in the Chemistry department is highly appreciated.

REFERENCES

[1] Goncalves, M.Guerreiro, M. C. Ramos, P. H.de Oliveira, L. C.Sapag, K., *Activated carbon prepared from coffee pulp: potential adsorbent of organic contaminants in aqueous solution.* Water Sci Technol, 2013. 68(5): p. 1085-90.

[2] Kaur, M. and M. Datta, *Adsorption Characteristics of Acid Orange 10 from Aqueous Solutions onto Montmorillonite Clay.* Adsorption Science & Technology, 2011. 29(3): p. 301-318.

[3] Negrulescu, A., *The Adsorption of Tartrazine, Congo Red and Methyl Orange on Chitosan Beads.* Digest Journal of Nanomaterials and Biostructures, 2014. 9(1): p. 45-52.

[4] Raha, S.Quazi, N.Ivanov, I. Bhattacharya, S.., *Dye/Clay intercalated nanopigments using commercially available non-ionic dye.* Dyes and Pigments, 2012. 93(1-3): p. 1512-1518.

[5] Kim, H. R.Jang, E.Kim, J.Joo, K. I.Lee, S. D.., *Dynamic polarization grating based on a dye-doped liquid crystal controllable by a single beam in a homeotropic-planar geometry.* Appl Opt, 2012. 51(36): p. 8526-34.

[6] Bernal, M.Romero, R.Roa, G.Barrera-Diaz, C.Torres-Blancas, T.Natividad, R., *Ozonation of Indigo Carmine Catalyzed with Fe-Pillared Clay.* International Journal of Photoenergy, 2013.

[7] Ma, J. Yu, F. Zhou, L. Jin, L. Yang, M. Luan, J.Tang, Y. Fan, H. Yuan, Z. Chen, J., *Enhanced adsorptive removal of methyl orange and methylene blue from aqueous solution by alkali-activated multiwalled carbon nanotubes.* ACS Appl Mater Interfaces, 2012. 4(11): p. 5749-60.

[8] Zhang, A.P. and Y. Fang, *Influence of adsorption orientation of methyl orange on silver colloids by Raman and fluorescence spectroscopy: pH effect.* Chemical Physics, 2006. 331(1): p. 55-60.

[9] Suciu, N. A. Ferrari, T.Ferrari, F. Trevisan, M. Capri, E.., *Pesticide removal from waste spray-tank water by organoclay adsorption after field application: an approach for a formulation of cyprodinil containing antifoaming/defoaming agents.* Environ Sci Pollut Res Int, 2012. 19(4): p. 1229-36.

[10] Li, C. S. Shi, X. F. Kao, S. J. Chen, M. T. Liu, Y. G. Fang, X. S. Lu, H. H. Zou, J. J. Liu, S. F. Qiao, S. Q., *Clay mineral composition and their sources for the fluvial sediments of Taiwanese rivers.* Chinese Science Bulletin, 2012. 57(6): p. 673-681.

[11] Du, J.Y., *Adsorption of fluoride on clay minerals and their mechanisms using X-ray photoelectron spectroscopy.*

Frontiers of Environmental Science & Engineering in China, 2011. 5(2): p. 212-226.

[12] Michalkova, A., T.L. Robinson, and J. Leszczynski, *Adsorption of thymine and uracil on 1: 1 clay mineral surfaces: comprehensive ab initio study on influence of sodium cation and water.* Physical Chemistry Chemical Physics, 2011. 13(17): p. 7862-7881.

[13] Rajkumar, K., A.L. Ramanathan, and P.N. Behera, *Characterization of clay minerals in the Sundarban mangroves river sediments by SEM/EDS.* Journal of the Geological Society of India, 2012. 80(3): p. 429-434.

[14] Srivastava, A.K., N. Khare, and P.S. Ingle, *Characterization of clay minerals in the sediments of Schirmacher Oasis, East Antarctica: their origin and climatological implications.* Current Science, 2011. 100(3): p. 363-372.

[15] Nasser, M.S., *Characterization of floc size and effective floc density of industrial papermaking suspensions.* Separation and Purification Technology, 2014. 122: p. 495-505.

[16] Novikova, L., *Characterization of Surface Acidity and Catalytic Ability of Natural Clay Minerals by Means of Test Catalytic Reaction.* Acta Geodynamica Et Geomaterialia, 2013. 10(4): p. 475-484.

[17] Tian, S.D., Y.Q. Zhuo, and C.H. Chen, *Characterization of the Products of the Clay Mineral Thermal Reactions during Pulverization Coal Combustion in Order to Study the Coal Slagging Propensity.* Energy & Fuels, 2011. 25(11): p. 4896-4905.

[18] Ozkan, I., M. Colak, and R.E. Oyman, *Characterization of waste clay from the Sardes (Salihli) placer gold mine and its utilization in floor-tile manufacture.* Applied Clay Science, 2010. 49(4): p. 420-425.

[19] Perri, F., *Chemical and minero-petrographic features of Plio-Pleistocene fine-grained sediments in Calabria, southern Italy.* Italian Journal of Geosciences, 2014. 133(1): p. 101-115.

[20] Kiesel, I., *Temperature-driven adsorption and desorption of proteins at solid-liquid interfaces.* Langmuir, 2014. 30(8): p. 2077-83.

[21] Ho, y.-s., *Review of second order models for adsorption systems.* hazadous material, 2006. B136: p. 681-689.

[22] Geersen, J., *The 2004 Aceh-Andaman Earthquake: Early clay dehydration controls shallow seismic rupture.* Geochemistry Geophysics Geosystems, 2013. 14(9): p. 3315-3323.

[23] Dharmendra, K., *Aceclofenac delivery by microencapsulation using LBL self-assembly for delayed release.* Pak J Pharm Sci, 2011. 24(4): p. 495-502.

[24] Jinamoni, S. and S.G. Archana, *Arsenic removal, from water by adsorption utilizing natural kaolinite clay of Assam.* Research Journal of Chemistry and Environment, 2011. 15(2): p. 559-563.

[25] de Araujo, A.L.P., *A Kinetic and Equilibrium Study of Zinc Removal by Brazilian Bentonite Clay.* Materials Research-Ibero-American Journal of Materials, 2013. 16(1): p. 128-136.

[26] Lee, C.R., *Pseudo first-order adsorption kinetics of N719 dye on TiO2 surface.* ACS Appl Mater Interfaces, 2011. 3(6): p. 1953-7.

[27] Joseph, K.M. and B.T. Christelle, *Removal of Mercury (II) ions from Aqueous Solutions using Granular Activated Carbon (GAC) and Kaolinite Clay from Mayouom in Cameroon: Kinetics and Equilibrium studies.* Research Journal of Chemistry and Environment, 2010. 14(3): p. 60-65.

[28] Diaz Gomez-Trevino, A.P., V. Martinez-Miranda, and M. Solache-Rios, *Removal of remazol yellow from aqueous solutions by unmodified and stabilized iron modified clay.* Applied Clay Science, 2013. 80-81: p. 219-225.

[29] Dridi-Dhaouadi, S., N. Ben Douissa-Lazreg, and M.F. M'Henni, *Removal of lead and yellow 44 acid dye in single and binary component systems by raw Posidonia oceanica and the cellulose extracted from the raw biomass.* Environ Technol, 2011. 32(3-4): p. 325-40.

[30] Szlachta, M. and P. Wojtowicz, *Adsorption of methylene blue and Congo red from aqueous solution by activated carbon and carbon nanotubes.* Water Sci Technol, 2013. 68(10): p. 2240-8.

[31] Yao, Y.J., *Equilibrium and kinetic studies of methyl orange adsorption on multiwalled carbon nanotubes.* Chemical Engineering Journal, 2011. 170(1): p. 82-89.

[32] Ferrero, F., C. Tonetti, and M. Periolatto, *Adsorption of chromate and cupric ions onto chitosan-coated cotton gauze.* Carbohydr Polym, 2014. 110: p. 367-73.

[33] Chen, S.H.Z., J. Zhang, C. L. Yue, Q. Y. Li, Y. Li, C., *Equilibrium and kinetic studies of methyl orange and methyl violet adsorption on activated carbon derived from Phragmites australis.* Desalination, 2010. 252(1-3): p. 149-156.

[34] Ai, L.H., C.Y. Zhang, and L.Y. Meng, *Adsorption of Methyl Orange from Aqueous Solution on Hydrothermal Synthesized Mg-Al Layered Double Hydroxide.* Journal of Chemical and Engineering Data, 2011. 56(11): p. 4217-4225.

[35] Ma, Q.L.S., F. F.Lu, X. F.Bao, W. R.Ma, H. Z., *Studies on the adsorption behavior of methyl orange from dye wastewater onto activated clay.* Desalination and Water Treatment, 2013. 51(19-21): p. 3700-3709.

[36] Yao, Y.J.H., B. Xu, F. F. Chen, X. F., *Equilibrium and kinetic studies of methyl orange adsorption on multiwalled carbon nanotubes.* Chemical Engineering Journal, 2011. 170(1): p. 82-89.

[37] Mittal, A., *Studies on the adsorption kinetics and isotherms for the removal and recovery of Methyl Orange from wastewaters using waste materials.* Journal of Hazardous Materials, 2007. 148(1-2): p. 229-240.

[38] Peng Liu, L.Z., *Adsorption of dyes from aqueous solutions or suspensions with clay nano-adsorbents.* Journal of separation purification technology, 2007. 58: p. 32-39.